JOURNAL OF COMPUTATIONAL PHYSICS **134,** 332–341 (1997)
ARTICLE NO. CP975711

A Numerical Scheme for Transport Equations with Spatially Distributed Coefficients Based on Locally Exact Difference Method

Katsuhiro Sakai* and Gen Sheng Zhang

Department of Electrical Engineering, Saitama Institute of Technology, 1690 Fusaiji, Okabecho, Saitama, 369-02 Japan

Received May 20, 1996; revised March 28, 1997

A numerical difference scheme to solve stationary transport equations with spatially distributed coefficients is presented. The spatial distribution of the coefficients in the transport equations is taken into consideration based on a four-region model among three adjacent control volumes, in which continuous conditions for solutions are imposed on the boundary between two adjacent regions. The coefficients in the difference scheme are determined so that it will be satisfied exactly by any local solution of the continuous equations with piecewise constant coefficients in each region. The present scheme is examined through numerical experiments for one-dimensional convection–diffusion equations with spatially distributed coefficients and source term and a two-dimensional cavity flow problem. The present scheme shows good solutions.

1. INTRODUCTION

So far strenuous efforts have been made to develop high-order numerical schemes for transport equations with the convection term. The difficulty in devising a high-accuracy scheme exists a conflicting requirements of accuracy on one hand and stability on the other. While the stability usually requires some kind of diffusive smoothing mechanism, the accuracy relies precisely on the opposite [1].

Linear high-order schemes [2–6] with constant difference coefficients based on polynomial differencing such as the QUICK scheme [5] tend to give rise to unphysical oscillations (numerical oscillations), especially in regions of steep gradients. This difficulty has been overcome by the use of artificial viscosity such as FCT [7] and FRAM [8] techniques. Furthermore, total variation diminishing flux limiters (TVD) [9] and high-resolution flux limiters [1, 10] to suppress the local oscillations have been proposed.

Alternatively, the concept of locally exact numerical differencing was introduced by Allen and Southwell [11], upon which numerical schemes involving three points in a one-dimensional field were developed [12]. Beyond these, LECUSSO (locally exact consistent upwind schemes of second order) [13] were proposed. Versions of LECUSSO have been proposed, which are formulated in conservation form for uniform mesh size grids [14] and for nonuniform mesh sizes [15].

Those locally exact schemes are characterized by determining difference coefficients so that the resulting difference equation will satisfy locally the exact solution of the convection–diffusion equation with constant coefficients. The difference coefficients depend on local velocities. The locally exact schemes have been extended to transport equations with absorption [16, 17] and source terms [18, 19]. In most cases numerical experiments with these locally exact schemes have shown stable and good solutions [15, 17].

However, in those locally exact schemes, the coefficients of the transport equations are assumed to be (local) constants between adjacent control volumes. Beyond this the source term is also treated as a constant. Therefore, it is preferable to construct a numerical scheme, taking into consideration the spatial distributions of the coefficients, inclusive of the absorption and the source term in the transport equations, especially when the coefficients vary steeply, such as the neutron transport equation with strong absorption near the control rods in a nuclear reactor.

In this study, spatial distribution of the coefficients in transport equations is taken into consideration, based on a four-region model among three adjacent control volumes in a staggered computational grid with nonuniform mesh sizes, in which the continuous conditions for the locally exact solution in each region are imposed on the boundary between two adjacent regions. Thus a new scheme, SDCLENS (spatially distributed coefficients locally exact numerical scheme), is constructed on the basis of the locally exact solutions consistent with spatially piecewise coefficients of the transport equations among three adjacent control volumes. The present scheme has been examined through numerical experiments for both one- and two-dimensional transport equations.

* Corresponding author.

0021-9991/97 $25.00

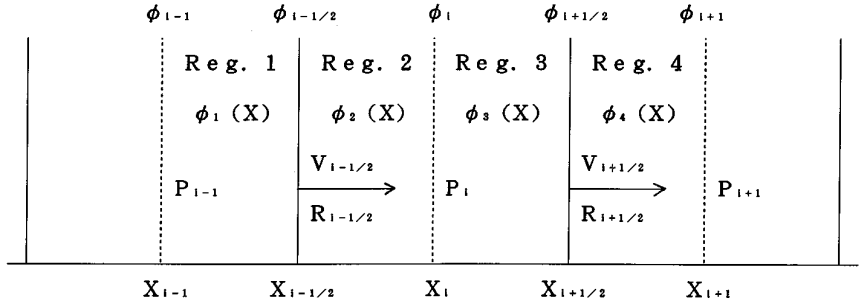

FIG. 1. Four-region model in a staggered computational grid.

2. MATHEMATICAL FORMULATION

To begin with, we outline our mathematical procedures. The essence of the method is to choose the coefficients in the difference scheme so that it will be satisfied exactly by any local solution of the continuous equations, that is, a solution of the continuous equations with piecewise constant coefficients and quadratic source term. The first step, therefore, is to find a general form for the local solution of the continuous equations in terms of a particular solution plus two solutions of the homogeneous equation. Requiring that the resulting difference scheme be satisfied exactly for these three solutions determines the three coefficients in the difference scheme. Having determined the coefficients in the difference scheme, the transport equation can then be solved by a straightforward matrix inversion.

2.1. Transport Equations

We consider a one-dimensional, stationary state transport equation,

$$\frac{d^2\phi}{dx^2} - R(x)\frac{d\phi}{dx} - P(x)\phi + Q(x) = 0, \tag{1}$$

where ϕ is the transported quantity and x denotes the Cartesian space coordinate. $R(x)$, $P(x)$, and $Q(x)$ denote the intensity of the convection, absorption, and source normalized by the diffusion parameters such as the kinematic viscosity ν. In this section, discussions on mathematical treatments of the spatial distribution of $R(x)$, $P(x)$, and $Q(x)$ are focussed.

2.2. Difference Formula

Here we consider a staggered-mesh grid with nonuniform mesh sizes, in which the transporting velocities are located on the control volume surface and other properties such as the transported quantity ϕ and the intensity of absorption P are defined at the control volume center, as shown in Fig. 1. This staggered-mesh grid is usually used in the field of computational fluid dynamics. We approximate the convection term in Eq. (1) at $x = x_i$ as

$$\left.\frac{d\phi}{dx}\right|_i = \frac{(\phi_{i+1/2} - \phi_{i-1/2})}{\Delta x_i}. \tag{2}$$

Here $\phi_{i+1/2}$ and $\phi_{i-1/2}$, the transported quantities defined on the control volume surfaces, are approximated on the basis of upwind differencing by the expressions:

$$\phi_{i+1/2} = A_{i+1/2}\phi_{i-1} + B_{i+1/2}\phi_i + C_{i+1/2}\phi_{i+1} \quad \text{for } R_{i+1/2} > 0, \tag{3.a}$$

$$= A_{i+1/2}\phi_i + B_{i+1/2}\phi_{i+1} + C_{i+1/2}\phi_{i+2} \quad \text{for } R_{i+1/2} < 0, \tag{3.b}$$

$$\phi_{i-1/2} = A_{i-1/2}\phi_{i-2} + B_{i-1/2}\phi_{i-1} + C_{i-1/2}\phi_i \quad \text{for } R_{i-1/2} > 0, \tag{3.c}$$

$$= A_{i-1/2}\phi_{i-1} + B_{i-1/2}\phi_i + C_{i-1/2}\phi_{i+1} \quad \text{for } R_{i-1/2} < 0. \tag{3.d}$$

Hereafter we assume $R_{i+1/2} > 0$ and $R_{i-1/2} > 0$.

The next step is to determine the difference coefficients ($A_{i+1/2}$, $B_{i+1/2}$, $C_{i+1/2}$) in Eq. (3). In Ref. [19], we already derived those coefficients for the transport equation with constant coefficients R and P and quadratic source $Q(x)$, namely based on a one-region model. Here we derive a locally exact difference formula, taking into consideration the spatial distribution of the coefficients R and P based on a four-region model.

In Fig. 1, we refer to Reg. 1 for the region between x_{i-1} and $x_{i-1/2}$, Reg. 2 for the region between $x_{i-1/2}$ and x_i, Reg. 3 for the region between x_i and $x_{i+1/2}$, and Reg. 4 for the region $x_{i+1/2}$ and x_{i+1}, respectively. P_{i-1}, P_i, and P_{i+1} are used in Reg. 1, in Regs. (2 and 3), and in Reg. 4, respectively. Hereafter subscript k indicates the region number associated with the control volume i under consideration, as shown in Fig. 1, and the mixed number such as $(i + k)$ and $(i + k + 1/2)$ indicates the location of the x-coordinate.

Based on this four-region model, we consider the continuous equation with piecewise coefficients R and P and quadratic source $Q(x)$ in each region $k = 1$–4 associated with the control volume i as follows:

$$\frac{d^2\phi}{dx^2} - R_{i-1/2}\frac{d\phi}{dx} - P_{i+k-2}\phi + Q(x) = 0 \quad \text{for } k = 1, 2, \quad (4.a)$$

$$\frac{d^2\phi}{dx^2} - R_{i+1/2}\frac{d\phi}{dx} - P_{i+k-3}\phi + Q(x) = 0 \quad \text{for } k = 3, 4. \quad (4.b)$$

The general solutions for Eq. (4) are given by (on Reg. k)

$$\phi_{i,k}(x) = \phi^0_{i,k}(x) + \phi^p_{i,k}(x) \quad \text{for } k = 1, 2, 3, 4, \quad (5)$$

where $\phi^0_{i,k}(x)$ is the homogeneous solution without the source term and $\phi^p_{i,k}(x)$ is the particular solution. $\phi^0_{i,k}(x)$ is given by

$$\phi^0_{i,k}(x) = E_{k,1}\exp[\omega_{k,1}x] + E_{k,2}\exp[\omega_{k,2}x] \quad \text{for } k = 1, 2, 3, 4, \quad (6)$$

where $E_{k,1}$ and $E_{k,2}$ are constants determined by boundary conditions and $\omega_{k,1}$, and $\omega_{k,2}$ are the roots of the following characteristic equations:

$$\omega^2 - R_{i-1/2}\omega - P_{i+k-2} = 0 \quad \text{for } k = 1, 2, \quad (7.a)$$

$$\omega^2 - R_{i+1/2}\omega - P_{i+k-3} = 0 \quad \text{for } k = 3, 4. \quad (7.b)$$

Here we assume $\omega_{k,1} \neq \omega_{k,2}$ without loss of generality. If the roots of Eq. (6) are imaginary numbers, the exponential functions in Eq. (6) are to be replaced by the trigonometrical functions. The expression of Eq. (6) may generally include such a case of the trigonometric functions. When the source $Q(x)$ is given as a second-order polynomial by

$$Q(x) = a_0 + a_1x + a_2x^2, \quad (8)$$

we have

$$\phi^p_{i,k}(x) = d_{k,0} + d_{k,1}x + d_{k,2}x^2 + d_{k,3}x^3, \quad (9)$$

where for $k = 1$ and 2 and $P_{i+k-2} \neq 0$

$$d_{k,0} = \frac{a_0}{P_{i+k-2}} - \frac{R_{i-1/2}(a_1P_{i+k-2} - 2a_2R_{i-1/2})}{(P_{i+k-2})^3} + \frac{2a_2}{(P_{i+k-2})^2},$$

$$d_{k,1} = -\frac{2a_2R_{i-1/2}}{(P_{i+k-2})^2} + \frac{a_1}{P_{i+k-2}}, \quad d_{k,2} = \frac{a_2}{P_{i+k-2}}, \quad d_{k,3} = 0;$$

for $k = 1$ and 2 and $P_{i+k-2} = 0$

$$d_{k,0} = \text{arbitrary constant},$$

$$d_{k,1} = \frac{a_1R_{i-1/2} + 2a_2 + a_0(R_{i-1/2})^2}{(R_{i-1/2})^3},$$

$$d_{k,2} = \frac{a_1R_{i-1/2} + 2a_2}{(R_{i-1/2})^2}, \quad d_{k,3} = \frac{a_2}{3R_{i-1/2}}.$$

$\phi^p_{i,k}(x)$ for $k = 3$ and 4 is given by replacing P_{i+k-2} and $R_{i-1/2}$ in the above equations with P_{i+k-3} and $R_{i+1/2}$, respectively. When the values Q_{i-1}, Q_i, and Q_{i+1} of $Q(x)$ at $x = x_{i-1}$, x_i, and x_{i+1}, respectively, are known in actual calculations, the polynomial Eq. (9) for $Q(x)$ can be obtained by an interpolation technique in terms of those three values of $Q(x)$.

In Eq. (6), eight constants $E_{k,1}$ and $E_{k,2}$ for $k = 1, 2, 3$, and 4 can be reduced to two constants by imposing the continuous conditions at $x = x_{i-1/2}$, $x = x_i$, and $x = x_{i+1/2}$. At $x = x_{i-1+k/2}$ for $k = 1, 2, 3$,

$$\phi_{i,k} = \phi_{i,k+1}, \quad \phi'_{i,k} = \phi'_{i,k+1}, \quad (10)$$

where the superscript $'$ denotes the derivative with respect to x.

From Eq. (10) we obtain

$$E_{k,1} = \alpha_{k,1}E_{k-1,1} + \alpha_{k,2}E_{k-1,2} + \alpha_{k,3} \quad \text{for } k = 2, 3, 4, \quad (11.a)$$

$$E_{k,2} = \beta_{k,1}E_{k-1,1} + \beta_{k,2}E_{k-1,2} + \beta_{k,3} \quad \text{for } k = 2, 3, 4, \quad (11.b)$$

where

$$\alpha_{k,1} = \frac{(\omega_{k-1,1} - \omega_{k,2})\exp[\omega_{k-1,1}x_{i-1+k/2}]}{(\omega_{k,1} - \omega_{k,2})\exp[\omega_{k,1}x_{i-1+k/2}]}, \quad (12.a)$$

$$\alpha_{k,2} = \frac{(\omega_{k-1,2} - \omega_{k,2})\exp[\omega_{k-1,2}x_{i-1+k/2}]}{(\omega_{k,1} - \omega_{k,2})\exp[\omega_{k,1}x_{i-1+k/2}]}, \quad (12.b)$$

$$\alpha_{k,3} = \frac{\{\phi^p_{i,k-1}{}'(x_{i-1+k/2}) - \phi^p_{i,k}{}'(x_{i-1+k/2}) - \omega_{k,2}[\phi^p_{i,k-1}(x_{i-1+k/2}) - \phi^p_{i,k}(x_{i-1+k/2})]\}}{(\omega_{k,1} - \omega_{k,2})\exp[\omega_{k,1}x_{i-1+k/2}]}, \quad (12.c)$$

$$\beta_{k,1} = \frac{(\omega_{k-1,1} - \omega_{k,1})\exp[\omega_{k-1,1}x_{i-1+k/2}]}{(\omega_{k,2} - \omega_{k,1})\exp[\omega_{k,2}x_{i-1+k/2}]}, \quad (13.a)$$

$$\beta_{k,2} = \frac{(\omega_{k-1,2} - \omega_{k,1})\exp[\omega_{k-1,2}x_{i-1+k/2}]}{(\omega_{k,2} - \omega_{k,1})\exp[\omega_{k,2}x_{i-1+k/2}]}, \quad (13.b)$$

$$\beta_{k,3} = \frac{\{\phi^p_{i,k-1}{}'(x_{i-1+k/2}) - \phi^p_{i,k}{}'(x_{i-1+k/2}) - \omega_{k,1}[\phi^p_{i,k-1}(x_{i-1+k/2}) - \phi^p_{i,k}(x_{i-1+k/2})]\}}{(\omega_{k,2} - \omega_{k,1})\exp[\omega_{k,2}x_{i-1+k/2}]}. \quad (13.c)$$

In the same manner as Ref. [19], we impose that Eq. (3.a) satisfy the exact solution Eq. (5) of Eq. (4). Substituting Eq. (5) into Eq. (3.a) yields

$$\begin{aligned} &E_{3,1}\exp[\omega_{3,1}x_{i+1/2}] + E_{3,2}\exp[\omega_{3,2}x_{i+1/2}] + \phi^p_{i,3}(x_{i+1/2}) \\ &= A_{i+1/2}(E_{1,1}\exp[\omega_{1,1}x_{i-1}] + E_{1,2}\exp[\omega_{1,2}x_{i-1}] + \phi^p_{i,1}(x_{i-1})) \\ &\quad + B_{i+1/2}(E_{2,1}\exp[\omega_{2,1}x_i] + E_{2,2}\exp[\omega_{2,2}x_i] + \phi^p_{i,2}(x_i)) \\ &\quad + C_{i+1/2}(E_{4,1}\exp[\omega_{4,1}x_{i+1}] + E_{4,2}\exp[\omega_{4,2}x_{i+1}] + \phi^p_{i,4}(x_{i+1})). \end{aligned} \quad (14)$$

Expressing $E_{k,1}$, $E_{k,2}$ for $k = 2, 3, 4$ in Eq. (14) with $E_{1,1}$ and $E_{1,2}$ by using Eq. (11) and rearranging Eq. (14) in respect to $E_{1,1}$ and $E_{1,2}$, we require that Eq. (14) identically hold for arbitrary values of $E_{1,1}$ and $E_{1,2}$. From this requirement, we obtain the matrix equation (see Appendix)

$$\mathbf{M} \cdot \begin{vmatrix} A_{i+1/2} \\ B_{i+1/2} \\ C_{i+1/2} \end{vmatrix} = \mathbf{N}, \tag{15}$$

where the matrices $\mathbf{M} = [M_{m,n}]$, $\mathbf{N} = [N_m]$ are defined as follows:

$$\begin{aligned}
M_{1,1} &= \exp[\omega_{1,1} x_{i-1}], \\
M_{1,2} &= \alpha_{2,1} \exp[\omega_{2,1} x_i] + \beta_{2,1} \exp[\omega_{2,2} x_i], \\
M_{1,3} &= (\alpha_{4,1}\alpha_{3,1}\alpha_{2,1} + \alpha_{4,1}\alpha_{3,2}\beta_{2,1} \\
&\quad + \alpha_{4,2}\beta_{3,1}\alpha_{2,1} + \alpha_{4,2}\beta_{3,2}\beta_{2,1}) \exp[\omega_{4,1} x_{i+1}] \\
&\quad + (\beta_{4,1}\alpha_{3,1}\alpha_{2,1} + \beta_{4,1}\alpha_{3,2}\beta_{2,1} \\
&\quad + \beta_{4,2}\beta_{3,1}\alpha_{2,1} + \beta_{4,2}\beta_{3,2}\beta_{2,1}) \exp[\omega_{4,2} x_{i+1}], \\
M_{2,1} &= \exp[\omega_{1,2} x_{i-1}], \\
M_{2,2} &= \alpha_{2,2} \exp[\omega_{2,1} x_i] + \beta_{2,2} \exp[\omega_{2,2} x_i], \\
M_{2,3} &= (\alpha_{4,1}\alpha_{3,1}\alpha_{2,2} + \alpha_{4,1}\alpha_{3,2}\beta_{2,2} \\
&\quad + \alpha_{4,2}\beta_{3,1}\alpha_{2,2} + \alpha_{4,2}\beta_{3,2}\beta_{2,2}) \exp[\omega_{4,1} x_{i+1}] \\
&\quad + (\beta_{4,1}\alpha_{3,1}\alpha_{2,2} + \beta_{4,1}\alpha_{3,2}\beta_{2,2} \\
&\quad + \beta_{4,2}\beta_{3,1}\alpha_{2,2} + \beta_{4,2}\beta_{3,2}\beta_{2,2}) \exp[\omega_{4,2} x_{i+1}], \\
M_{3,1} &= \phi^p_{i,1}(x_{i-1}), \\
M_{3,2} &= \alpha_{2,3} \exp[\omega_{2,1} x_i] + \beta_{2,3} \exp[\omega_{2,2} x_i] + \phi^p_{i,2}(x_i), \\
M_{3,3} &= (\alpha_{4,1}\alpha_{3,1}\alpha_{2,3} + \alpha_{4,1}\alpha_{3,2}\beta_{2,3} + \alpha_{4,2}\beta_{3,1}\alpha_{2,3} \\
&\quad + \alpha_{4,2}\beta_{3,2}\beta_{2,3} + \alpha_{4,1}\alpha_{3,3} + \alpha_{4,2}\beta_{4,3} + \alpha_{4,3}) \exp[\omega_{4,1} x_{i+1}] \\
&\quad + (\beta_{4,1}\alpha_{3,1}\alpha_{2,3} + \beta_{4,1}\alpha_{3,2}\beta_{2,3} + \beta_{4,2}\beta_{3,1}\alpha_{2,3} \\
&\quad + \beta_{4,2}\beta_{3,2}\beta_{2,3} + \beta_{4,1}\alpha_{3,3} + \beta_{4,2}\beta_{4,3} + \beta_{4,3}) \exp[\omega_{4,2} x_{i+1}] \\
&\quad + \phi^p_{i,4}(x_{i+1}); \\
N_1 &= (\alpha_{3,1}\alpha_{2,1} + \alpha_{3,2}\beta_{2,1}) \exp[\omega_{3,1} x_{i+1/2}] \\
&\quad + \beta_{3,1}\alpha_{2,1} + \beta_{3,2}\beta_{2,1}) \exp[\omega_{3,2} x_{i+1/2}], \\
N_2 &= (\alpha_{3,1}\alpha_{2,2} + \alpha_{3,2}\beta_{2,2}) \exp[\omega_{3,1} x_{i+1/2}] \\
&\quad + \beta_{3,1}\alpha_{2,2} + \beta_{3,2}\beta_{2,2}) \exp[\omega_{3,2} x_{i+1/2}], \\
N_3 &= (\alpha_{3,1}\alpha_{2,3} + \alpha_{3,2}\beta_{2,3}) \exp[\omega_{3,1} x_{i+1/2}] \\
&\quad + \beta_{3,1}\alpha_{2,3} + \beta_{3,2}\beta_{2,3}) \exp[\omega_{3,2} x_{i+1/2}] + \phi^p_{i,3}(x_{i+1/2}).
\end{aligned}$$

When the coefficients R and P are constant, we have $\phi^p_{i,k}(x) = \phi^p_{i,1}(x)$, $\omega_{k,1} = \omega_{1,1}$, $\omega_{k,2} = \omega_{1,2}$ for $k = 1$ to 4, and $\alpha_{k,1} = \beta_{k,2} = 1$, $\alpha_{k,2} = \alpha_{k,3} = \beta_{k,1} = \beta_{k,3} = 0$ for $k = 1$ to 4. Then from Eq. (15), we obtain

$$\begin{aligned}
&\begin{vmatrix} \exp[\omega_1 x_{i-1}] & \exp[\omega_1 x_i] & \exp[\omega_1 x_{i+1}] \\ \exp[\omega_2 x_{i-1}] & \exp[\omega_2 x_i] & \exp[\omega_2 x_{i+1}] \\ \phi^p_{i,1}(x_{i-1}) & \phi^p_{i,1}(x_i) & \phi^p_{i,1}(x_{i+1}) \end{vmatrix} \begin{vmatrix} A_{i+1/2} \\ B_{i+1/2} \\ C_{i+1/2} \end{vmatrix} \\
&\quad = \begin{vmatrix} \exp[\omega_1 x_{i+1/2}] \\ \exp[\omega_1 x_{i+1/2}] \\ \phi^p_{i,1}(x_{i+1/2}) \end{vmatrix}.
\end{aligned} \tag{16}$$

with $\omega_1 = \omega_{k,1}$ and $\omega_2 = \omega_{k,2}$ for $k = 1$ to 4. Equation (16) is identical to Eq. (15) in Ref. [19]. From Eq. (15), we obtain the difference coefficients $A_{i+1/2}$, $B_{i+1/2}$, and $C_{i+1/2}$.

The stability analysis for the above scheme using the characteristic polynomial analysis method performed by the author [20, 21] was carried out for the convection–diffusion equation with constant coefficients and absorption. The results show that the present locally exact scheme, taking into consideration the absorption term, has the non-oscillation properties, while the locally exact schemes, without consideration of the absorption term such as the LECUSSO scheme, may show oscillatory solutions.

3. NUMERICAL EXPERIMENTS

Here we perform numerical experiments to examine the present scheme by using one- and two-dimensional problems.

3.1. One-Dimensional Problem

3.1.1. *Computational Conditions*

The transport equation for the first experiment is

$$\begin{aligned}
&\frac{d^2\phi}{dx^2} + \tan(x)\frac{d\phi}{dx} \\
&\quad + (K\cos(x))^2\phi + \cos^2(x)\cos(K\sin(x)) = 0,
\end{aligned} \tag{17}$$

with $R(x) = -\tan(x)$, $P(x) = -(K\cos(x))^2$, and $Q(x) = \cos^2(x)\cos(K\sin(x))$ in Eq. (1). We solve Eq. (17) with the uniform mesh $\Delta x = \pi/40$, in which the total mesh number n and the total computational length XT are 20 and $\pi/2$, respectively. K is a nonzero parameter. In this experiment, the transporting velocity is everywhere negative and its absolute values go up to infinity near the right side boundary $x = \pi/2$. The boundary values at $x = 0$ and $x = \pi/2$ are set to $\phi(0) = \phi_1 = 1.0$ and $\phi(\pi/2) = \phi_n =$

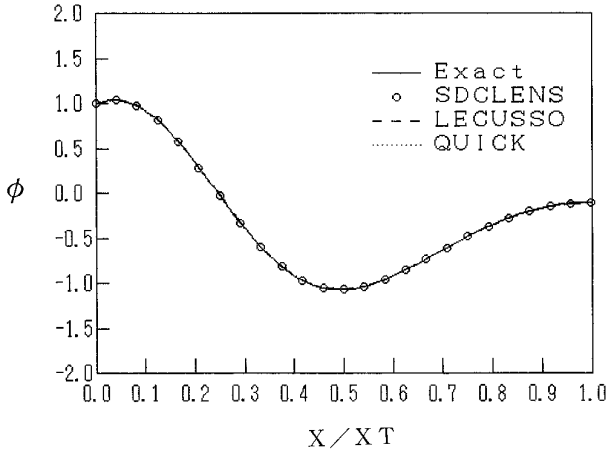

FIG. 2. Comparison of numerical solutions with the analytical solution for $K = 5$.

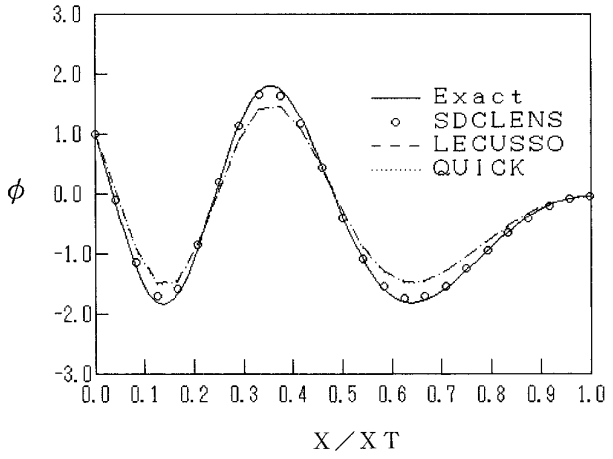

FIG. 3. Comparison of numerical solutions with the analytical solution for $K = 10$.

$\sin(K)/2K$, respectively. The analytical solution is given by using an intermediate variable as

$$\phi(x) = \cos(K\sin(x)) - \cot(K)\sin(K\sin(x)) + \sin(x)\sin(K\sin(x))/2K. \tag{18}$$

This experiment is preferable to validate the present scheme since the coefficients of this test equation are strongly dependent on the space coordinate when K is large.

3.1.2. *Numerical Solutions*

Discretizing the convection term and the diffusion term in Eq. (17) with Eqs. (2), (3.b), and (3.d), and the second-order central scheme, respectively, we obtain the difference equation

$$\begin{aligned}&(\phi_{i+1} - 2\phi_i + \phi_{i-1})\\ &- Rm_i\{[A_{i+1/2}\phi_i + B_{i+1/2}\phi_{i+1} + C_{i+1/2}\phi_{i+2}]\\ &- [A_{i-1/2}\phi_{i-1} + B_{i-1/2}\phi_i + C_{i-1/2}\phi_{i+1}]\}\\ &- P(x_i)\,\Delta x_i^2\phi_i + Q(x_i)\,\Delta x_i^2 = 0 \quad \text{for } i = 2, 3, ..., n-2,\end{aligned} \tag{19}$$

with $Rm_i = (R_{i-1/2} + R_{i+1/2})\,\Delta x_i/2$. Since $R(x) = -\tan(x)$ is negative everywhere in the computational region, $\phi_{i+1/2}$ and $\phi_{i-1/2}$ are evaluated by Eq. (3.b) and Eq. (3.d), respectively. At $i = n - 1$, we use the analytical solution. We obtain the numerical solution ϕ_i ($i = 2$–$n - 2$) by solving the matrix equation $\mathbf{G}\cdot[\phi] = \mathbf{H}$, where $\mathbf{G}$ and $\mathbf{H}$ are $(n-3)\times(n-3)$ and $(n-3)\times 1$ matrices produced by Eq. (19), respectively.

3.1.3. *Comparison of Numerical and Analytical Solutions*

Figures 2, 3, and 4 show the comparison of numerical solutions by the present SDCLENS, LECUSSO, and QUICK schemes with the analytical solution for $K = 5$, $K = 10$, and $K = 15$, respectively. All the numerical solutions for small values of K less than about 5 are in good agreement with the analytical solution. The spatial dependence of the absorption term $P(x)$ and source term $Q(x)$ in this test equation increases with the increase of K. In Fig. 7 for $K = 15$, the solution with the present SDCLENS scheme is distinctly better than solutions with the locally exact schemes LECUSSO based on a one-region model and Taylor expansion scheme QUICK.

3.2. Two-Dimensional Problem

We solve the recirculating stationary flow driven by combined shear and body forces in a two-dimensional square

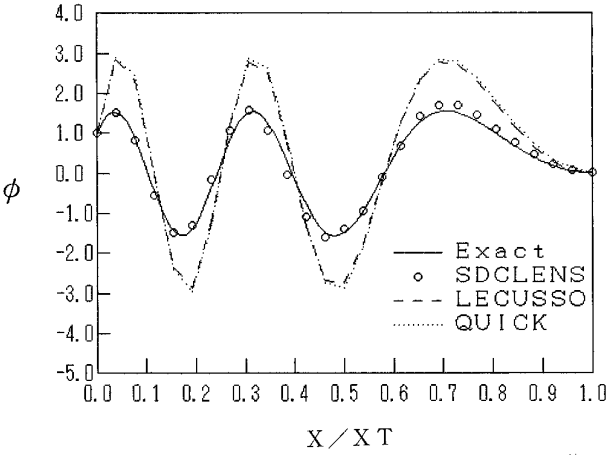

FIG. 4. Comparison of numerical solutions with the analytical solution for $K = 15$.

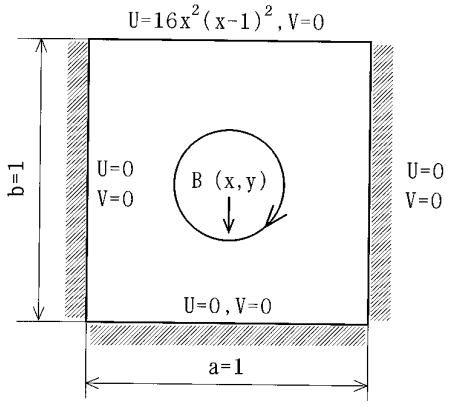

FIG. 5. Two-dimensional driven cavity.

cavity shown in Fig. 5, which was constructed by Shih *et al*. [22]. The exact solution of this flow problem is known.

3.2.1. *Computational Conditions*

The governing equations in terms of vorticity ω and stream function ψ for the above cavity flow are

$$u\frac{\partial\omega}{\partial x}+v\frac{\partial\omega}{\partial y}=\nu\left[\frac{\partial\omega}{\partial x^2}+\frac{\partial\omega}{\partial y^2}\right]-\frac{\partial B}{\partial x}, \tag{20}$$

$$\frac{\partial\psi}{\partial x^2}+\frac{\partial\psi}{\partial y^2}=-\omega, \tag{21}$$

$$u=\frac{\partial\psi}{\partial y},\quad v=-\frac{\partial\psi}{\partial x}, \tag{22}$$

$$\omega=\frac{\partial v}{\partial x}-\frac{\partial u}{\partial y}. \tag{23}$$

The body force B is present in the y-direction. The expression for B is lengthy and is given in Ref. [22].

The boundary conditions for the velocities u and v are of Dirichlet type, zero everywhere, except along the top surface ($y = 1$), where $v(x, y) = 0$ and

$$u(x,1)=16x^2(x-1)^2. \tag{24}$$

The boundary condition for ω on the wall is evaluated with the second-order accuracy.

The analytical solutions for the stream function and velocities are

$$\phi(x,y)=8x^2(x-1)^2y^2(y^2-1), \tag{25}$$

$$u(x,y)=16x^2(x-1)^2y^2(2y^2-1), \tag{26}$$

$$v(x,y)=-16x(x-1)(2x-1)y^2(y^2-1). \tag{27}$$

3.2.2. *Numerical Method*

The above governing equations are solved with the uniform mesh grids 20×20. The convection terms in those equations are discretized by Eq. (3) and the diffusion terms are discretized with the second-order central scheme. The discretized equation for Eq. (20) is solved as an initial value problem by using a time marching method, and Eq. (21) is solved by the SOR method.

The difference coefficients ($A_{i\pm1/2}$, $B_{i\pm1/2}$, $C_{i\pm1/2}$) in Eqs. (3.a)–(3.d) are determined independently in each x- and y-direction on the basis of the four-region model in Section 2. Further, we have tried to include coupling effects between x- and y-directions, but regrettably we could not obtain converged solutions. The method to determine those coefficients with the coupling effect is explained below. After the coefficients are determined, those coefficients are employed to solve the discretized equations for the governing equations. Namely, the method explained below is not to solve the governing equations but merely an approximate method to determine the difference coefficients with coupling effects between the two dimensions.

By analogy with the factorisation method, we separate Eq. (30) into two parts as

$$\nu\frac{\partial\omega}{\partial x^2}-u\frac{\partial\omega}{\partial x}-\alpha\omega=0, \tag{28}$$

$$\nu\frac{\partial\omega}{\partial y^2}-v\frac{\partial\omega}{\partial y}+\alpha\omega-g=0, \tag{29}$$

with $g = \partial B/\partial x$. α is a kind of separation parameter and is to be determined by the iterative calculation as explained later. Since the source term $g(x, y)$ in Eq. (29) depends on x and y, the rigorous factorisation technique is not applicable to get solutions. But we apply this technique only to get the difference coefficients ($A_{i\pm1/2}$, $B_{i\pm1/2}$, $C_{i\pm1/2}$). Any solution of Eqs. (28) and (29) satisfies Eq. (20).

The difference coefficients in both x- and y-directions are evaluated using Eqs. (28) and (29) on the basis of the four-region model. Then α is approximately estimated by using older values of the velocities, the vorticity, and the difference coefficients in the iterative calculations:

$$\begin{aligned}\alpha^x=\Big[&-u_{i,j}\,\Delta x\{[A^x_{i+1/2,j}\omega_{i,j}+B^x_{i+1/2,j}\omega_{i+1,j}+C^x_{i+1/2,j}\omega_{i+2,j}]\\&-[A^x_{i-1/2,j}\omega_{i-1,j}+B^x_{i-1/2,j}\omega_{i,j}+C^x_{i-1/2,j}\omega_{i+1,j}]\}\\&+\nu(\omega_{i+1,j}-2\omega_{i,j}+\omega_{i-1,j})\Big]/(\omega_{i,j}\,\Delta x^2),\end{aligned} \tag{30.a}$$

$$\begin{aligned}\alpha^y=\Big[&v_{i,j}\,\Delta y\{[A^y_{i,j+1/2}\omega_{i,j}+B^y_{i,j+1/2}\omega_{i,j+1}+C^y_{i,j+1/2}\omega_{i,j+2}]\\&-[A^y_{i,j-1/2}\omega_{i,j-1}+B^y_{i,j-1/2}\omega_{i,j}+C^y_{i,j-1/2}\omega_{i,j+1}]\}\\&-\nu(\omega_{i,j+1}-2\omega_{i,j}+\omega_{i,j-1})+g_{i,j}\,\Delta y^2\Big]/(\omega_{i,j}\,\Delta y^2),\end{aligned} \tag{30.b}$$

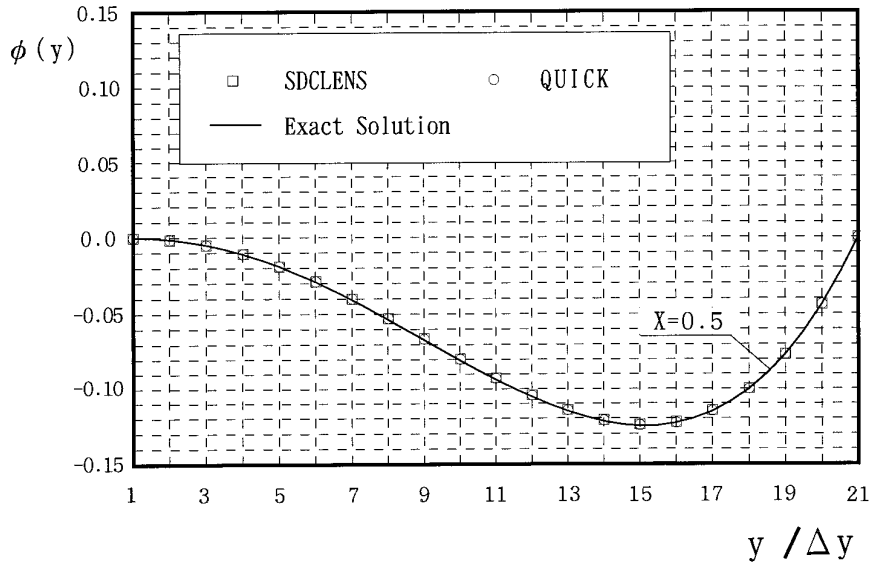

FIG. 6. Comparison of numerical solutions with the analytical solution for the stream function $\phi(0.5, y)$ along the y-directional line of symmetry at Re = 1.

$$\alpha_{i,j} = (\alpha^x + \alpha^y)/2. \tag{31}$$

Since we could not obtain converged solutions by using the above procedure, we evaluated independently the difference coefficients ($A^x_{i\pm1/2,j}$, $B^x_{i\pm1/2,j}$, $C^x_{i\pm1/2,j}$, $A^y_{i,j\pm1/2}$, $B^y_{i,j\pm1/2}$, $C^y_{i,j\pm1/2}$) in both x- and y-directions based on the four-region model from Eqs. (28) and (29) with $\alpha = 0$, respectively. Then we solve the governing equations. Further investigation on the coupling effects between the two dimensions are necessary for multidimensional equations.

3.2.3. *Comparison of Numerical and Analytical Solutions*

Figures 6 and 7 show the comparison of numerical solutions by the present SDCLENS and QUICK schemes with the exact solution for the stream function $\phi(0.5, y)$ and x-component of velocities $u(0.5, y)$ along the y-directional

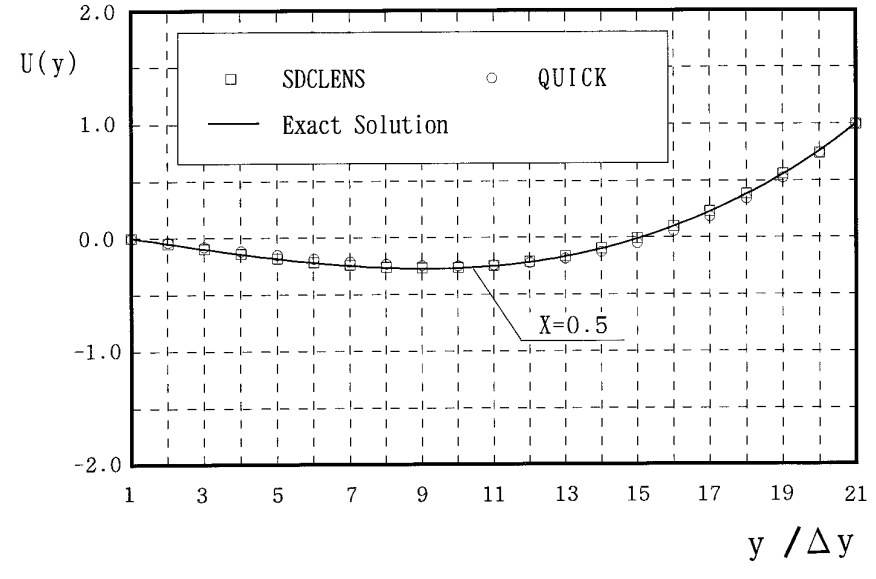

FIG. 7. Comparison of numerical solutions with the analytical solution for the x-component of velocities $u(0.5, y)$ along the y-directional line of symmetry at Re = 1.

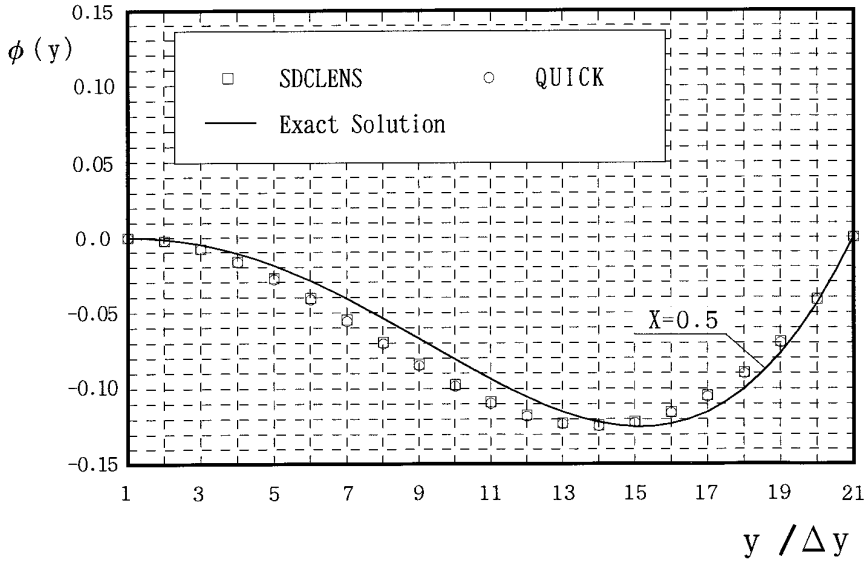

FIG. 8. Comparison of numerical solutions with the analytical solution for the stream function $\phi(0.5, y)$ along the y-directional line of symmetry at Re = 100.

line of symmetry at Re = $1/\nu = 1$. Figures 8 and 9 show the same comparison at Re = 100.

Both the numerical solutions with the SDCLENS and QUICK schemes at Re = 1 are in good agreement with the exact solution. At Re = 100, the SDCLENS scheme shows globally the solutions a little better, as compared with the QUICK scheme, but there exist no significant differences between these two solutions, on the contrary, to the first experiment. This may be due to the fact that the velocity $u(0.5, y)$ at $x = 0.5$ does not so strongly vary along the y-direction, as compared with the coefficients in Eq. (17).

Finally, we compare the computational efficiency of the present scheme with the linear scheme QUICK. The cpu time consumed to get stationary solutions by the SDCLENS scheme on the computer VT-Alpha433AXP

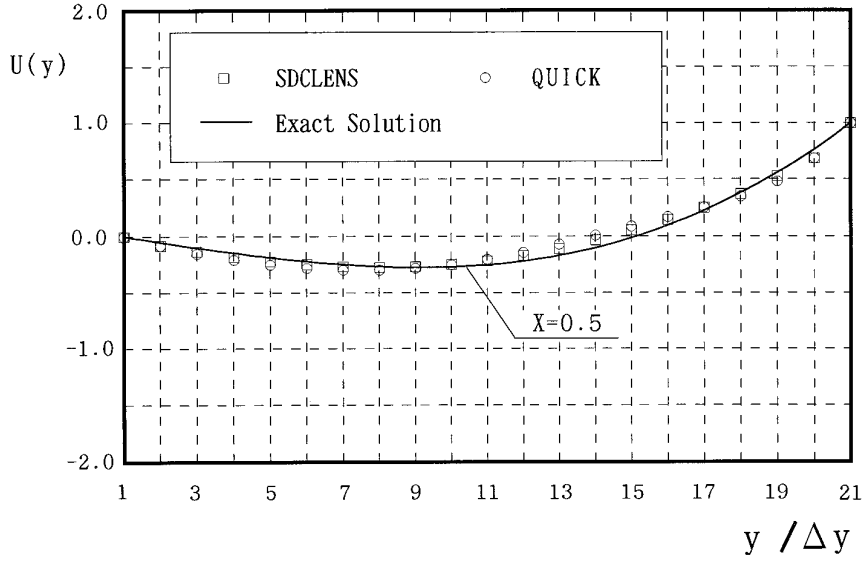

FIG. 9. Comparison of numerical solutions with the analytical solution for the x-component of velocities $u(0.5, y)$ along the y-directional line of symmetry at Re = 100.

was 121 s, which was about 50 times that using the QUICK scheme. The number of steps required for the time-marching iterative calculations were same for both calculations with the SDCLENS and the QUICK schemes. The cpu time for the SDCLENS was dominated by the solution of Eq. (15). In case we use the first-order upwind scheme in the beginning, hundreds of steps for the time-marching iterative calculations, the cpu time could be decreased to almost one-half without making changes on the converged solutions. Hence in the practical application of the present scheme to stationary equations, there may exist an efficient iterative method by appropriately combining the SDCLENS and the first-order upwind schemes. The cpu time depends on a programming technique, especially in this complicated algorithm as compared with the linear QUICK scheme with constant difference coefficients. The present SDCLENS program has not been always optimized.

4. CONCLUSIONS

A new numerical scheme SDCLENS (spatially distributed coefficients locally exact numerical scheme) for the convection term in transport equations was presented in which the difference coefficients are determined such that the resulting equation interpolating numerical fluxes satisfies any locally exact solution of the transport equations with absorption and source terms. The spatial distribution of the coefficients of the transport equations was taken into consideration based on a four-region model among three adjacent control volumes, in which continuous conditions of solutions are imposed on each boundary between two adjacent regions. Thus the SDCLENS scheme is constructed on the basis of the locally exact solutions, consistent with the spatially piecewise coefficients of the transport equations in the frame of a four-region model.

The SDCLENS scheme was examined through numerical experiments using the one-dimensional transport equation with spatially distributed coefficients and the two-dimensional cavity flow problem. The present SDCLENS scheme showed good solutions, as compared with the conventional locally exact scheme LECUSSO and Taylor expansion scheme QUICK schemes. The cpu time consumed by the SDCLENS scheme was about 50 times of that by the QUICK scheme. Further investigations on the coupling effects between the two dimensions are necessary for two-dimensional equations.

APPENDIX

This appendix outlines the derivation of Eq. (15), which is able to be easily extended to a general N-region model. When we improve the interpolation formula Eq. (3) with four or five base points (four or five difference coefficients A, B, C, D, etc. in Eq. (3)), a general N-region model is preferable, in which we need one or two more independent relations among the difference coefficients such as relations to guarantee the first-order accuracy and the second-order accuracy.

Equation (11) can be expressed by the matrix in the homogeneous form

$$\begin{vmatrix} E_{k,1} \\ E_{k,2} \\ 1 \end{vmatrix} = \mathbf{T}_k \cdot \begin{vmatrix} E_{k-1,1} \\ E_{k-1,2} \\ 1 \end{vmatrix} \quad \text{for } k = 2, 3, 4, \tag{A.1}$$

where

$$\mathbf{T}_k \equiv \begin{vmatrix} \alpha_{k,1} & \alpha_{k,2} & \alpha_{k,3} \\ \beta_{k,1} & \beta_{k,2} & \beta_{k,3} \\ 0 & 0 & 1 \end{vmatrix}. \tag{A.2}$$

By using Eq. (A.1), we obtain

$$\begin{vmatrix} E_{k,1} \\ E_{k,2} \\ 1 \end{vmatrix} = \prod_{m=2}^{k} \mathbf{T}_m \cdot \begin{vmatrix} E_{1,1} \\ E_{1,2} \\ 1 \end{vmatrix} \quad \text{for } k = 2, 3, 4. \tag{A.3}$$

Equation (14) can be expressed by the matrix form

$$\begin{aligned} &A_{i+1/2}(\exp[\omega_{1,1}x_{i-1}]\exp[\omega_{1,2}x_{i-1}]\,\phi_1^p(x_{i-1}))(E_{1,1}\,E_{1,2}\,1)^{\mathrm{t}} \\ &\quad + B_{i+1/2}(\exp[\omega_{2,1}x_i]\exp[\omega_{2,2}x_i]\,\phi_2^p(x_i))(E_{2,1}\,E_{2,2}\,1)^{\mathrm{t}} \\ &\quad + C_{i+1/2}(\exp[\omega_{4,1}x_{i+1}]\exp[\omega_{4,2}x_{i+1}]\,\phi_4^p(x_{i+1}))(E_{4,1}\,E_{4,2}\,1)^{\mathrm{t}} \\ &= (\exp[\omega_{3,1}x_{i+1/2}]\exp[\omega_{3,2}x_{i+1/2}]\,\phi_3^p(x_{i+1/2}))(E_{3,1}\,E_{3,2}\,1)^{\mathrm{t}}, \end{aligned} \tag{A.4}$$

where the superscript t denotes transposed matrix. Expressing $(E_{k,1}\ E_{k,2}\ 1)^{\mathrm{t}}$ for $k = 2, 3, 4$ with $(E_{1,1}\ E_{1,2}\ 1)^{\mathrm{t}}$ by using Eq. (A.3) and substituting those into (A.4) yields

$$\begin{aligned} &A_{i+1/2}(\exp[\omega_{1,1}x_{i-1}]\exp[\omega_{1,2}x_{i-1}]\,\phi_1^p(x_{i-1}))(E_{1,1}\,E_{1,2}\,1)^{\mathrm{t}} \\ &\quad + B_{i+1/2}(\exp[\omega_{2,1}x_i]\exp[\omega_{2,2}x_i]\,\phi_2^p(x_i))\mathbf{T}_2(E_{1,1}\,E_{1,2}\,1)^{\mathrm{t}} \\ &\quad + C_{i+1/2}(\exp[\omega_{4,1}x_{i+1}]\exp[\omega_{4,2}x_{i+1}]\,\phi_4^p(x_{i+1}))\mathbf{T}_4(E_{1,1}\,E_{1,2}\,1)^{\mathrm{t}} \\ &= (\exp[\omega_{3,1}x_{i+1/2}]\exp[\omega_{3,2}x_{i+1/2}]\,\phi_3^p(x_{i+1/2}))\mathbf{T}_3(E_{1,1}\,E_{1,2}\,1)^{\mathrm{t}}, \end{aligned} \tag{A.5}$$

By imposing that Eq. (A.5) hold identically for any value of $E_{1,1}$ and $E_{1,2}$, we obtain

$$
\begin{aligned}
&A_{i+1/2}(\exp[\omega_{1,1}x_{i-1}]\exp[\omega_{1,2}x_{i-1}]\,\phi_1^p(x_{i-1}))\\
&\quad + B_{i+1/2}(\exp[\omega_{2,1}x_i]\exp[\omega_{2,2}x_i]\,\phi_2^p(x_i))\mathbf{T}_2\\
&\quad + C_{i+1/2}(\exp[\omega_{4,1}x_{i+1}]\exp[\omega_{4,2}x_{i+1}]\,\phi_4^p(x_{i+1}))\mathbf{T}_4\\
&\quad - (\exp[\omega_{3,1}x_{i+1/2}]\exp[\omega_{3,2}x_{i+1/2}]\,\phi_3^p(x_{i+1/2}))\mathbf{T}_3 = (0\,0\,0).
\end{aligned}
\tag{A.6}
$$

From Eq. (A.6), we obtain three equations and reach Eq. (15).

When we improve the numerical accuracy of the scheme with four difference coefficients such as

$$
\begin{aligned}
\phi_{i+1/2} = {} & A_{i+1/2}\phi_{i+1} + B_{i+1/2}\phi_i\\
& + C_{i+1/2}\phi_{i-1} + D_{i+1/2}\phi_{i-2},
\end{aligned}
\tag{A.7}
$$

we may use another relation to guarantee the first-order accuracy as follows:

$$
\begin{aligned}
x_{i+1/2} = {} & A_{i+1/2}x_{i+1/2} + B_{i+1/2}x_i\\
& + C_{i+1/2}x_{i-1} + D_{i+1/2}x_{i-2}.
\end{aligned}
\tag{A.8}
$$

REFERENCES

1. M. S. Darwish, A new high-resolution scheme based on the normalized variable formulation, *Numer. Heat Transfer, Part B* **24,** 353 (1993).
2. M. Atias *et al*., Efficiency of Navier–Stokes solvers, *AIAA J.* **15**(2), 263 (1977).
3. B. P. Leonard, A stable and accurate convective modelling procedure based on quadratic upstream interpolation, *Comput. Methods Appl. Mech. Engrg.* **19,** 59 (1979).
4. J. K. Dukowicz and J. D. Ramshaw, Tensor–viscosity method for convection in numerical fluid dynamics, *J. Comput. Phys.* **32,** 71 (1979).
5. B. P. Leonard, Finite difference method IV, in *Handbook of Numerical Heat Transfer*, edited by W. J. Minkowycz *et al.* (Wiley, New York, 1988), Chap. 9, p. 347.
6. T. Kawamura and K. Kuwahara, Computation of high Reynolds number flow around a circular cylinder with surface roughness, AIAA-84-0340, 1984.
7. J. P. Boris and D. L. Book, Flux-corrected transport 1. SHASTA, a fluid transport algorithm that works, *J. Comput. Phys.* **11,** 38 (1973).
8. M. Chapman, FRAM nonlinear damping algorithms for the continuity equation, *J. Comput. Phys.* **44,** 84 (1981).
9. A. Harten, High resolution scheme for hyperbolic conservation laws, *J. Comput. Phys.* **49,** 357 (1983).
10. B. P. Leonard, Simple high-accuracy resolution program for comvective modelling of discontinuities, *Int. J. Numer. Meth. Eng.* **8,** 1291 (1988).
11. D. N. de Allen and R. V. Southwell, Relaxation methods applied to determine the motion, in two dimensions, of a viscous fluid past a fixed cylinder, *J. Mech. Appl. Math.* **8,** 129 (1955).
12. D. B. Spalding, A novel finite difference formulation for differential expressions involving both first and second derivatives, *Int. J. Numer. Methods Eng.* **4,** 551 (1972).
13. C. Günther, A consistent upwind method of the locally exact consistent upwind scheme of second order, in *Computational Techniques and Applications CTAC-87*, edited by J. Noye and C. Fletcher (Elsevier Science, North-Holland, Amsterdam, 1988), p. 249.
14. Cl. Günther, Conservative versions of locally exact consistent upwind scheme of second order (LECUSSO-SCHEME), *Int. J. Numer. Methods Eng.* **34,** 793 (1992).
15. K. Sakai, Conservative LECUSSO scheme in nonuniform mesh size grids—Numerical experiments and natural circulation test analysis, *Comput. Fluid Dyn. J.* **1**(1), 34 (1992).
16. M. Carroll and J. J. H. Miller, Completely exponentially fitted finite difference schemes for some singular perturbation problems, in *Computational and Asymptotic Methods* (Boole Press, Doublin, 1980), p. 225.
17. Cl. Günther, Locally exact upwind difference schemes for convection-diffusion equations with absorption, *Z. Angew. Math. Mech.* **72,** T521 (1992).
18. C. Prakash, Application of the locally analytic differencing scheme to some test problems for the convection-diffusion equation, *Numer. Heat Transfer* **7,** 165 (1984).
19. K. Sakai, Locally exact numerical scheme for transport equations with source terms—LENS, *J. Nucl. Sci. Tech.* **29**(8), 824 (1992).
20. K. Sakai, Numerical oscillations analysis on high-order LECUSSO scheme based on characteristic polynomial technique, *J. At. Energy Soc. Japan* **34**(6), 544 (1992). [Japanese]
21. K. Sakai, A new finite variable difference method with application to locally exact numerical difference scheme, *J. Comput. Phys.* **124,** 391 (1996).
22. T. M. Shih and C. H. Tan, Effects of grid staggering on numerical schemes, *Internat. J. Numer. Methods Fluids* **9,** 193 (1989).